Electron-capture decay of ^{206}Po†

L. J. Jardine* and A. A. Shihab-Eldin‡
University of California, Lawrence Berkeley Laboratory, Berkeley, California 94720
(Received 27 January 1975)

The energies and intensities of 77 γ-ray transitions assigned to the electron-capture decay of ^{206}Po have been measured. Multipolarities of transitions were determined from internal conversion coefficients calculated from our relative γ-ray intensities and the relative conversion electron intensities of Fujika, Kanbe, and Hisatake. γ-ray singles, γ-γ coincidence, and previous conversion electron measurements were used to construct a more complete decay scheme for ^{206}Po. Data obtained from in-beam reaction studies, ^{210}At α decay studies, and the present electron-capture decay scheme were used to identify states in ^{206}Bi of a one proton particle-three neutron hole character. In addition a qualitative discussion of the level structure of ^{206}Bi generated from (zero-order) couplings of $1h_{9/2}$ and $2f_{7/2}$ protons with the low-lying states of ^{205}Pb is given, and this is compared with reasonable success to the experimental spectrum. The dominant electron-capture decay rates are explained in terms of an allowed single-particle mechanism.

[RADIOACTIVITY ^{206}Po [from ^{209}Bi(p, $4n$)]; measured E_γ, I_γ, γ-γ coin; deduced EC branching, logft. ^{206}Bi deduced levels, J, π, γ multipolarity. Ge(Li) detectors, Ge(Li)-Ge(Li) coin.]

I. INTRODUCTION

The ^{206}Bi nucleus can be described in terms of the shell model as one proton particle and three neutron holes removed from the doubly closed shell of ^{208}Pb. The low-lying level structure of ^{206}Bi is expected to be generated from the couplings of $1h_{9/2}$ and $2f_{7/2}$ protons with the low-lying three neutron hole states in ^{205}Pb. Allowed electron-capture decay from the 0^+ ground state of ^{206}Po is expected to directly populate only the 1^+ states of ^{206}Bi. Subsequent electromagnetic transition cascades to the 6^+ ground state of ^{206}Bi should populate states in the spin range of 0–7, thus identifying a major portion of the 1p-3h states in ^{206}Bi.

Earlier investigations of the electron-capture decay of ^{206}Po were carried out by Arbman[1] and Stoner[2] before high-resolution Ge(Li) detectors were available. More recent in-beam reaction studies[3,4] have provided some properties of the high-spin states of ^{206}Bi. Direct measurements of the α spectra of ^{210}At have also been made.[5] To learn more about the level structure of ^{206}Bi, restudies of electromagnetic transitions from the electron-capture decay of ^{206}Po and from the α decay of ^{210}At were undertaken. Reports[6,7] of the α decay of ^{210}At have been given elsewhere. During the course of the electron-capture study,[8] preliminary reports[9] on the internal-conversion electrons from the ^{206}Po decay were made available to us. These high-resolution magnetic spectrometer measurements prompted us to abandon Si(Li) conversion-electron measurements and to concentrate on γ-ray singles and γ-γ coincidence measurements in order to further establish the decay scheme.

In this paper we report the γ-ray transitions following the electron-capture decay of ^{206}Po using Ge(Li) spectrometers. A new decay scheme for ^{206}Po is constructed from present and all previous data.[1-9] The levels of ^{206}Bi are discussed in terms of a zero-order one proton particle-three neutron hole coupling model.

II. EXPERIMENTAL

A. Source preparation

Sources of 8.8-day ^{206}Po were obtained by the reaction ^{209}Bi(p, $4n$)^{206}Po at bombarding energies of 37–42 MeV with bismuth metal targets of thicknesses 25–115 mg/cm^2. These targets initially contained appreciable amounts of 5.7-h ^{207}Po and 2.9-yr ^{208}Po due to the broad excitaton functions for the (p, xn) reactions, so they were allowed to stand for several days until the ^{207}Po had decayed. The following modified chemical separation procedure[10] was used to remove the ^{207}Bi, in addition to the ^{206}Bi which grew in from the decay of ^{206}Po.

The target was dissolved in $6N$ HNO_3. The excess HNO_3 was destroyed by repeated additions of HCl followed by a slow evaporation of the solution to a small volume using a heat lamp. A 1 ml solution of the activity was made $\approx 0.3\,M$ in KI and $3\,M$ in HCl and then was transferred to a separatory funnel containing 5 ml of isopropyl ether. The polonium was extracted into the ether phase while the bismuth (and lead) remained in the aqueous phase. (A bismuth carrier was added when initial sources were "repurified" a second or third time after appreciable amounts of ^{206}Bi

has grown in.) The ^{206}Po was removed from the ether phase by washing with 3N HCl. Sources for γ-ray counting were prepared by evaporation onto thin aluminum or teflon backings.

B. Gamma ray spectra

γ-ray singles spectra were obtained with a 35-cm^3 coaxial Ge(Li) detector [system resolution 2.6 keV full width at half-maximum (FWHM) at 1332 keV] coupled with a 4096-channel data acquisition system previously described.[11,12] A 10-cm^3 planer Ge(Li) detector (system resolution 1.4 keV FWHM at 122 keV) was also used in some measurements. A typical γ-ray spectrum in the energy range of 30–1800 keV is shown in Fig. 1. Since ^{206}Bi, the daughter of ^{206}Po, was itself unstable to electron-capture decay, the γ-ray spectra became progessively more complex after the initial preparation of a ^{206}Po source. Thus, major ^{206}Bi γ rays are also identified in Fig. 1.

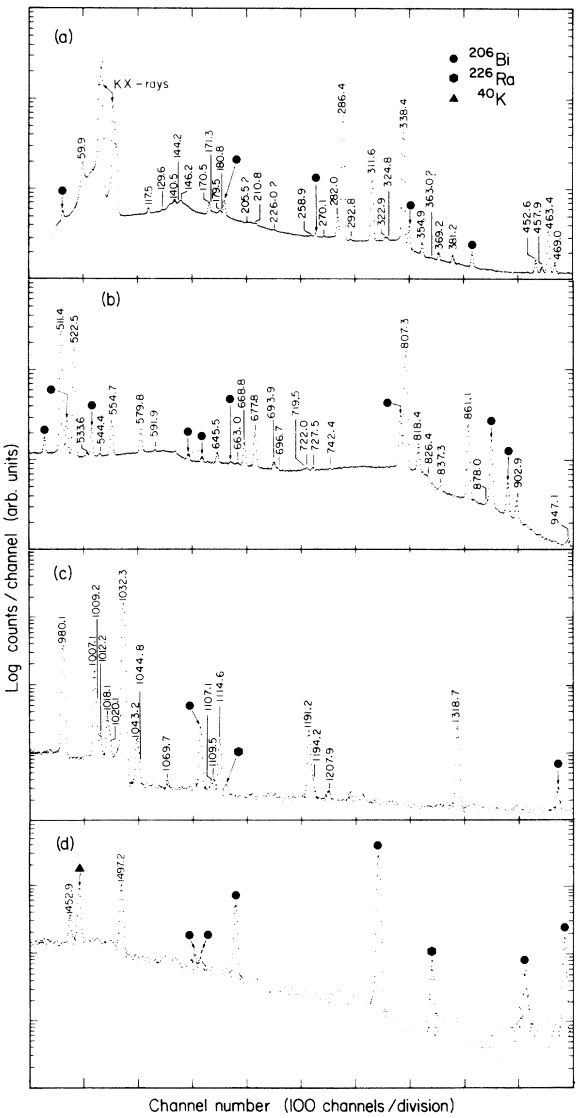

FIG. 1. Typical γ-ray spectrum of ^{206}Po. Transitions due to the decay of ^{206}Bi and background are labeled separately. Transitions not belonging to the decay of ^{206}Po are marked with symbols: ^{206}Bi=●, ^{226}Ra=⬢, ^{40}K=▲.

The spectra were analyzed with the computer code[13] SAMPO. Energy calibrations were obtained from the data compiled by Jardine.[14] Uncertainties due to relative efficiency calibrations[15] were estimated to be ± 5%. The energies and relative intensities of γ-ray transitions assigned to the decay of ^{206}Po are given in Table I, which also includes the energies of the transitions determined from the internal conversion-electron measurements of Ref. 9. Our results are in rather good agreement with those of Ref. 9 for transitions observed in both types of measurements. γ rays of energies $\lesssim$280 keV are especially difficult to observe because of the intense Compton background coupled with the relative weakness and complexity of these transitions. Thus the high-resolution conversion-electron energy measurements of Ref. 9 generally provide the most complete data below this energy.

We have also shown in Table I multipolarities for many γ rays which were deduced from a comparison of experimental subshell ratios and/or experimental conversion coefficients[9] with the theoretical values of Hager and Seltzer.[16] Conversion coefficients were calculated from the relative electron intensities of Ref. 9 and our relative γ-ray intensities; they were normalized to the theoretical value for the 861.1-keV $E2$ transition. A renormalization of the relative intensities in Table I can be made using the absolute intensity for the 286.2 keV γ ray calculated from the level scheme. It is calculated to be 22.8 ± 2.0 photons per 100 decays of ^{206}Po.

C. γ-γ coincidence measurements

Three parameter γ-γ coincidence measurements were made with two coaxial Ge(Li) detectors of about 35 cm^3 (active volume) each. The axes of the two detectors were positioned at 90° with respect to the source and were separated by a graded shield of lead-cadmium-copper to minimize scattering between the detectors. A fast-coincidence electronic arrangement (leading-edge timing) previously described[11,12] was used. The width of the prompt time distribution was determined from the 286 - 1032 keV γ-ray cascade to be about 35 nsec FWHM. Three parameter data ($E_1, E_2, \Delta t$) were stored serially on magnetic tape and were later sorted on the LBL CDC - 7600 com-

TABLE I. γ rays observed in the decay of ^{206}Po.

γ-ray[a] energy (keV)	γ-ray energy (keV)	Relative[b] γ-ray intensity	Multipolarity[c]
10.836 ± 0.022			$M1$
32.532 ± 0.019			$M1+E2$
53.610 ± 0.043			
50.908 ± 0.018	60.0 ± 0.3	4.6 ± 1.5	$E2$
82.802 ± 0.022			$M1$
109.484 ± 0.033			
117.536 ± 0.028	117.6 ± 0.2	0.40 ± 0.05	$M1$
124.669 ± 0.043			$(M1)$
129.644 ± 0.020	129.6 ± 0.3	0.10 ± 0.03	$M1$
140.486 ± 0.028	140.4 ± 0.6	0.40 ± 0.10	$M1$
144.166 ± 0.028	144.5 ± 0.6	0.15 ± 0.07	$M1$
146.180 ± 0.026	146.8 ± 0.6	0.31 ± 0.14	$M1$
152.308 ± 0.052			$(M1$
162.621 ± 0.030			
170.501 ± 0.021	170.6 ± 0.2	0.85 ± 0.34	$M1$
171.340 ± 0.024	171.5 ± 0.3	0.22 ± 0.12	$M1$
177.035 ± 0.036			
179.453 ± 0.020	179.1 ± 0.4	0.13 ± 0.08	$M1$
180.791 ± 0.019	180.6 ± 0.2	0.34 ± 0.15	$M1$
205.936 ± 0.050	205.5 ± 1.0[d]	0.16 ± 0.06	$(E2)$
210.672 ± 0.051	210.8 ± 0.2	0.15 ± 0.03	$(M1+E2)$
224.853 ± 0.042	226.0 ± 1.0[d]	0.065 ± 0.014	$(M1+E2)$
	258.9 ± 0.2	0.094 ± 0.013	
	270.1 ± 0.2	0.11 ± 0.02	
281.923 ± 0.023	282.0 ± 0.1	2.57 ± 0.16	$M1$
286.410 ± 0.026	286.4 ± 0.1	70.8 ± 3.9	$M1$
292.799 ± 0.030	292.8 ± 0.2	0.13 ± 0.02	$M1$
311.558 ± 0.030	311.6 ± 0.1	12.6 ± 0.8	$M1$
322.809 ± 0.033	322.9 ± 0.2	0.31 ± 0.03	$M1$
324.728 ± 0.040	324.8 ± 0.2	0.24 ± 0.03	$M1$
338.441 ± 0.034	338.4 ± 0.1	57.2 ± 3.0	$M1$
343.968 ± 0.041			$(M1)$
354.866 ± 0.037	354.9 ± 0.1	1.06 ± 0.05	$M1$
	363.0 ± 1.0[d]	0.10 ± 0.04	
369.077 ± 0.080	369.2 ± 0.1	0.60 ± 0.03	$M1$
381.220 ± 0.041	381.2 ± 0.1	0.57 ± 0.06	$M1$
452.472 ± 0.048	452.6 ± 0.2[e]	0.97 ± 0.07	$M1$
457.765 ± 0.049	457.9 ± 0.2	0.46 ± 0.03	$M1$
463.381 ± 0.048	463.4 ± 0.1	5.35 ± 0.30	$M1$
468.983 ± 0.052	469.0 ± 0.1	0.78 ± 0.04	$M1$
511.359 ± 0.052	511.4 ± 0.2	71.5 ± 3.8	$M1$
522.469 ± 0.052	522.5 ± 0.1	47.3 ± 2.5	$M1$
533.557 ± 0.063	533.6 ± 0.2	0.34 ± 0.03	$M1(+E2)$
544.393 ± 0.070	544.4 ± 0.2	0.23 ± 0.02	$M1(+E2)$
554.636 ± 0.056	554.7 ± 0.1	4.63 ± 0.24	$M1$
579.778 ± 0.060	579.8 ± 0.1	3.11 ± 0.16	$M1$
	591.9 ± 0.3	0.19 ± 0.02	
645.583 ± 0.067	645.5 ± 0.1	0.99 ± 0.06	$M1$
664.077 ± 0.077	663.0 ± 0.3	0.13 ± 0.02	$M1(+E2)$
668.750 ± 0.071	668.8 ± 0.1	2.57 ± 0.13	$M1$
677.709 ± 0.073	677.8 ± 0.1	4.37 ± 0.22	$E2$
693.812 ± 0.075	693.9 ± 0.2	0.64 ± 0.04	$M1(+E2)$
	696.7 ± 0.3[f]	0.12 ± 0.08	
719.699 ± 0.077	719.5 ± 0.3	0.15 ± 0.03	$M1$
722.034 ± 0.075	722.0 ± 0.4	0.22 ± 0.06	$M1$
	723.5 ± 1.2[g]	0.06 ± 0.05	
727.343 ± 0.078	727.5 ± 0.2	0.28 ± 0.03	$M1(+E2)$
	731.2 ± 1.0[g]	0.046 ± 0.023	

TABLE I *(Continued)*

γ-ray [a] energy (keV)	γ-ray energy (keV)	Relative [b] γ-ray intensity	Multipolarity [c]
	742.4 ± 0.5 [f]	0.086 ± 0.022	
807.385 ± 0.082	807.3 ± 0.1	67.9 ± 3.5	$M1$
818.231 ± 0.084	818.4 ± 0.2	3.33 ± 0.17	$E2$
826.442 ± 0.094	826.4 ± 0.2	0.21 ± 0.03	$M1$
837.235 ± 0.087	837.3 ± 0.2	0.34 ± 0.03	$M1$
860.933 ± 0.089	861.1 ± 0.2	10.2 ± 0.6	$E2$
866.225 ± 0.095			
	878.0 ± 0.2	0.21 ± 0.02	
902.531 ± 0.091	902.9 ± 0.3	0.75 ± 0.04	$E2$
947.241 ± 0.096	947.1 ± 0.3	0.11 ± 0.02	$M1(+E2)$
980.288 ± 0.096	980.1 ± 0.2	21.0 ± 1.1	$M1(+E2)$
1007.146 ± 0.097	1007.1 ± 0.2	9.00 ± 0.50	$M1$
1008.87 ± 0.10	1009.2 ± 0.4	0.62 ± 0.05	$M1(+E2)$
1012.23 ± 0.12	1012.2 ± 0.2	0.62 ± 0.04	$M1$
1017.93 ± 0.13	1018.1 ± 0.5 [e]	0.70 ± 0.06	$E2$
	1020.1 ± 0.3	0.47 ± 0.03	
1032.26 ± 0.10	1032.3 ± 0.2	(100)	$M1$
1043.17 ± 0.13	1043.2 ± 0.2	0.67 ± 0.06	$E2$
	1044.8 ± 0.3	0.37 ± 0.06	
	1069.7 ± 0.4	0.05 ± 0.01	
1105.25 ± 0.14			
	1107.1 ± 0.4 [g]	0.06 ± 0.02	
	1109.5 ± 0.3 [g]	0.08 ± 0.02	
1114.49 ± 0.14	1114.6 ± 0.2	0.92 ± 0.05	$M1$
1190.92 ± 0.14	1191.2 ± 0.2	1.42 ± 0.07	$E2$
1193.89 ± 0.16	1194.2 ± 0.3 [e]	0.14 ± 0.09	$M1$
	1207.9 ± 0.4 [g]	0.05 ± 0.04	
1318.68 ± 0.13	1318.7 ± 0.2	1.88 ± 0.10	$E2$
1452.74 ± 0.15	1452.9 ± 0.2	0.20 ± 0.02	$E2$
1496.70 ± 0.18	1497.2 ± 0.3 [e]	0.89 ± 0.05	$E2$
1566.40 ± 0.18	1566 ± 1 [g]	0.010 ± 0.010	
1571.02 ± 0.16			

[a] Energies were provided by Ref. 9.

[b] Absolute γ-ray intensities (derived from the level scheme) may be obtained by renormalizing the relative intensities, since the 286.4-keV transition has an absolute intensity of 22.8 ± 2.0 photons per 100 decays of ^{206}Po.

[c] Multipolarity deduced from internal conversion electron measurements of Ref. 9 as discussed in text.

[d] Peak may be complex.

[e] Intensity was corrected for a ^{206}Bi component.

[f] Intensity was corrected for a double or single escape peak component.

[g] Assignment to ^{206}Po decay from present data is very uncertain.

puter system. The sorting routine employed permitted subtraction of random events and events associated with the neighboring Compton distributions from each energy gate. Approximately 50 such sorts were performed at a resolving time of about 70 nsec. Several typical coincidence spectra are shown in Figs. 2 and 3. A summary of coincidence relations deduced from these measurements is given in Table II; it is based primarily on qualitative results. However, for several of the more intense γ rays for which multiple placements in the level scheme (Sec. III) were possible, spectra were analyzed in sufficient detail to establish a definite placement.

III. DECAY SCHEME

Coincidence measurements and sum-difference relationships among γ-ray energies have been used to construct the scheme shown in Fig. 4. Electron-capture branching ratios were determined from the total transition intensity (calculated from our γ-ray intensity data and the multipolarities given in Table I) depopulating each level.

No decay to the ground state was assumed. Based on the ^{206}Po electron-capture branching[17] of 94.6% and a Q value of 1820 ± 40 keV,[18] log ft values were calculated[19] employing the methods discussed by Konopinski and Rose.[20] Spin and parity assignments are based upon log ft values of electron-capture branches, γ-ray multipolarities, and previously reported data.[1-9] For completeness and for use in later discussions, levels populated by the α decay of ^{210}At[5,6] have also been included in Fig. 4.

The decay scheme of Fig. 4 is substantially different than the previous one proposed by Arbman[1] because of the discovery[9] of an intense (93% of EC decays) 10.84-keV $M1$ transition depopulating a new 3^+ state at 70.8 keV; this has been discussed recently in detail by Ref. 9. In the ^{206}Po decay, states of spin and parity 1^+ are directly populated, presumably by an allowed Gamow-Teller decay; states with spins $\lesssim 7$ are identified by subsequent γ-ray cascades to the 6^+ ground state.

IV. SPIN, PARITY, AND CONFIGURATION ASSIGNMENTS

No theoretical calculations of the level structure of ^{206}Bi have been made. However, its low-lying level structure might *a priori* be characterized by one (proton) particle-three (neutron) hole states arising from couplings of the (odd) 83rd

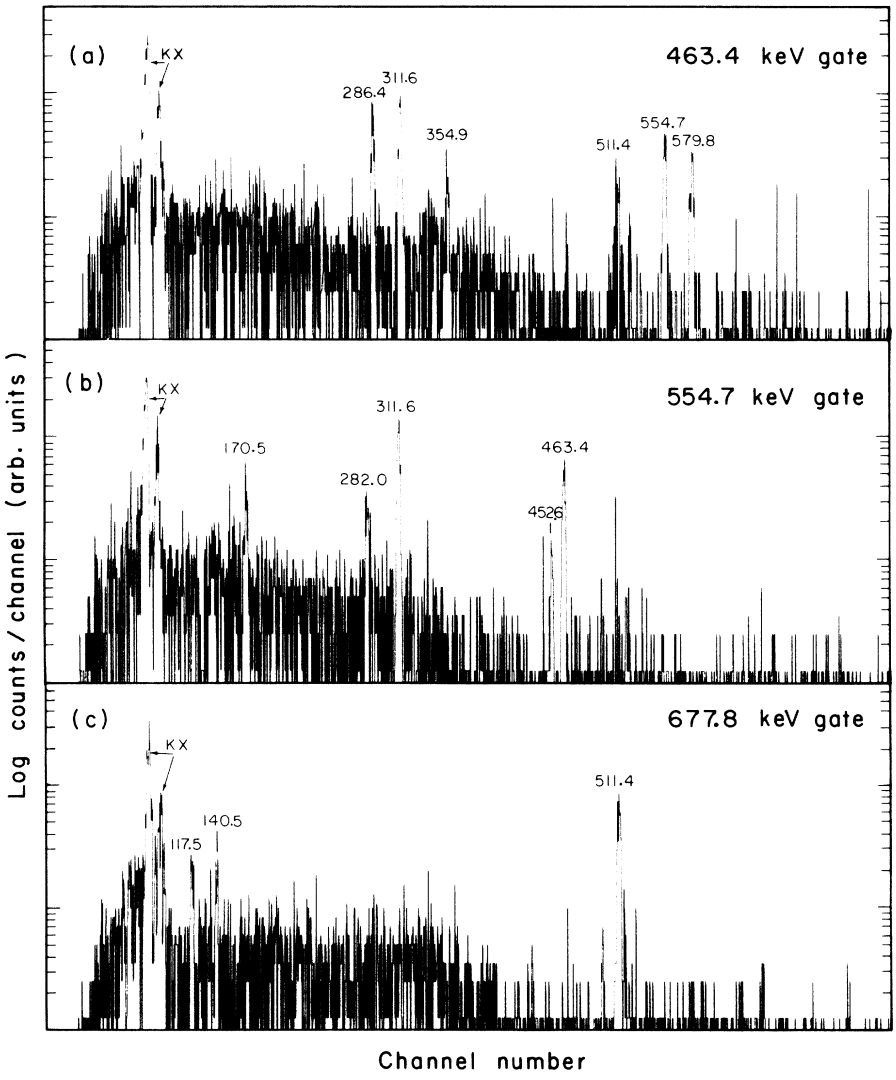

FIG. 2. γ-ray spectra in coincidence with the 463.4-, 554.7-, and 677.8-keV transitions. These helped establish levels at 523.3, 1078.0, and 878.1 keV, in addition to the placement of the 117.5- and 140.5-keV γ rays.

proton with the (odd) 123rd neutron. To estimate qualitatively the number and type of such states, we show in Fig. 5 the experimental[21-23] states of ^{209}Bi and ^{205}Pb. The first three states of ^{209}Bi are due[21] to the proton single-particle orbitals $1h_{9/2}$, $2f_{7/2}$, and $1i_{13/2}$. The four states of ^{205}Pb at 0, 2.3, 270, and 1014 keV are due[22] predominantly to an odd neutron (or three-neutron holes) in the $2f_{5/2}$, $3p_{1/2}$, $3p_{3/2}$, and $1i_{13/2}$ single-particle orbitals, respectively. The remaining ^{205}Pb states shown are presumably of a more complex nature. If one now considers couplings of the $1h_{9/2}$ and $2f_{7/2}$ protons with the three neutron hole states of ^{205}Pb, the band structure shown in column 4 of Fig. 5 results. For clarity, the degeneracy of multiplets formed from these couplings has not been removed; however, all possible spins contained in each multiplet are explicitly identified. For example, the ground state and other low-lying states of ^{206}Bi are presumably formed from the couplings of a $1h_{9/2}$ proton with an odd $2f_{5/2}$ neutron. The shell model configurations for such even parity states will be of the form $(\pi(h_{9/2})\nu(f_{5/2})^{-1}(p_{1/2})^{-2})_{J=2,3,4,5,6,7^+}$. Similarly, two states belonging to the $(\pi(h_{9/2})\nu(p_{1/2})^{-1}(f_{5/2})^{-2})_{4,5^+}$ configurations are expected in the immediate

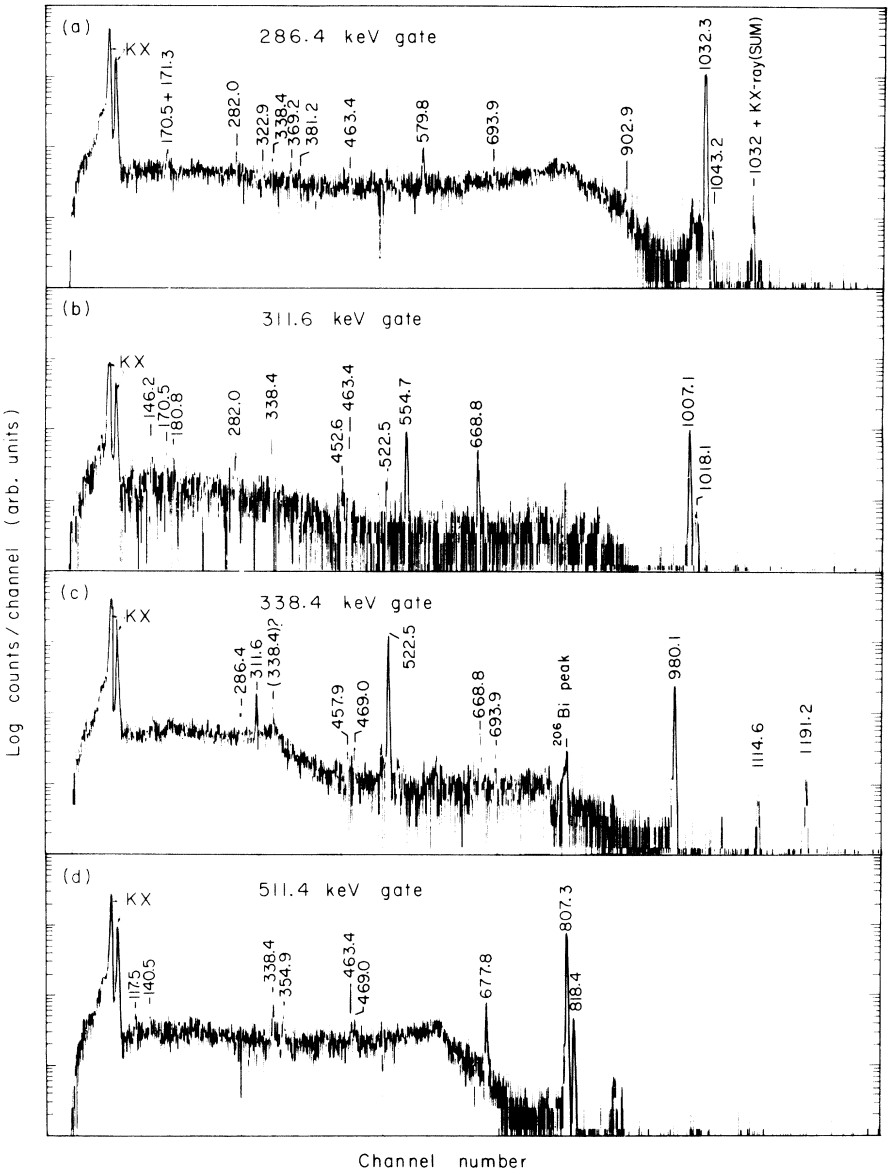

FIG. 3. γ-ray spectra in coincidence with the 286.4-, 311.6-, 338.4-, and 511.4-keV transitions.

TABLE II. γ-γ coincidence results.

E_γ (gate) (keV)	γ rays in coincidence with gate (keV)
170.5+ 171.3	K_X [a], 281.9, 286.4, 311.6, 554.7, 579.8
281.9	K_X, 170.5, 286.4, (311.6) [b], 381.3, 554.7, 579.8
286.4	K_X, 170.5, (171.3), 281.9, 322.9, (324.9), 338.5, 369.2, (381.3), 463.4, (522.6), 579.8, (694.0), 903.0, 1032.2, 1043.2
311.6	K_X, (146.2), (170.5), (180.8), 281.9, 338.5, 452.6, 463.4, 522.6, (544.4), 554.7, 668.8, (826.4), (837.3), (861.1), 1007.0, 1018.1
322.9	(554.7), (579.8)
338.5	K_X, 286.4, 311.6, (324.9), 457.9, 469.0, (511.4), 522.6, 668.8, 694.0, 980.1, 1114.6, 1191.2
354.9	K_X, (281.9), 463.4, 511.4
369.2	K_X, 286.4, (381.3)
452.6	K_X, (286.4), (311.6), (554.7), (579.8)
463.4	K_X, 286.4, 311.6, 354.9, 511.4, 554.7, 579.8, (1044.8)
469.0	K_X, 338.5, 511.4
511.4	K_X, 117.5, 140.5, 338.5, 354.9, 463.4, 469.0, 677.8, 807.3, 818.4
522.6	K_X, 338.6, 457.9
554.7	K_X, 170.5, 281.9, 311.6, (338?) [c], 452.6, 463.4
579.8	K_X, 170.5, (281.9), 286.4, (322.9), 452.6, 463.4
668.8	K_X, 311.6, 338.5
677.8	K_X, (83), 117.5, 140.5, 511.4
807.3	K_X, 511.4, (583.0), 645.5
818.4	K_X, 511.4
903.0	K_X, (140.5), 286.4
980.1	K_X, 338.5
861.1	K_X
1007.1+1009.2	K_X, 311.4
1018.1+1020.1	K_X, 311.4
1032.2	K_X, 286.4
1043.2+1044.8	K_X, 286.4, (463.4)
1107.1+1109.4	K_X, (286.4)
1114.6	K_X, 338.5
1191.2	K_X, 338.5
1194.2	K_X, 338.5
1318.7	K_X
1497.3	K_X

[a] K_X is used to mean K_α and K_β x rays of polonium.

[b] Energies in parentheses represent *possible* or weak coincidences.

[c] This coincidence would imply that a transition of 114.1 keV ($523.3 \xrightarrow{M1} 409.2$) exists; however, such a transition has not been observed.

proximity followed at a slightly higher energy by four states with the $(\pi(h_{9/2})\nu(p_{3/2})^{-1}(p_{1/2})^{-2})_{3,4,5,6^+}$ configurations. Finally all known experimental states of ^{206}Bi are shown (with a shifted energy for the ground state) in the last column of Fig. 5.

A. Levels at 0, 59.9, 70.8, 82.8, 140, and 409.2 keV

The ground state of ^{206}Bi has a measured spin[24] of 6 and can be assigned an even parity because of its shell-model configuration and electron-capture decay properties to states in ^{206}Pb. The α decay of ^{210}At populates[5] the ground state and a state at 60 keV. Arguments for the placement of a pure $E2$ transition deexciting a state at 59.9 keV have been given by Arbman[1]; this state has a measured[25] half-life of 7.8 ± 0.2 μsec. A spin of 4 for the 59.9-keV state is most consistent with the decay data and the lack of strong population of this state in in-beam reaction studies.[3,4]

A state at 70.8 keV is well defined by the decay scheme of Fig. 4. A 3^+ assignment for the spin and parity of this state can be made on the basis of the intense[9] 10.84-keV $M1$ transition depopulating this state to the 4^+ state at 59.9 keV and the 807.3-, 1007.1-, and 1032.3-keV $M1$ transitions populating this state from the 2^+ states at 878.1, 1078.0, and 1103.1 keV, respectively. The absence of α decay to this state, assuming such an assignment, is in agreement with detailed

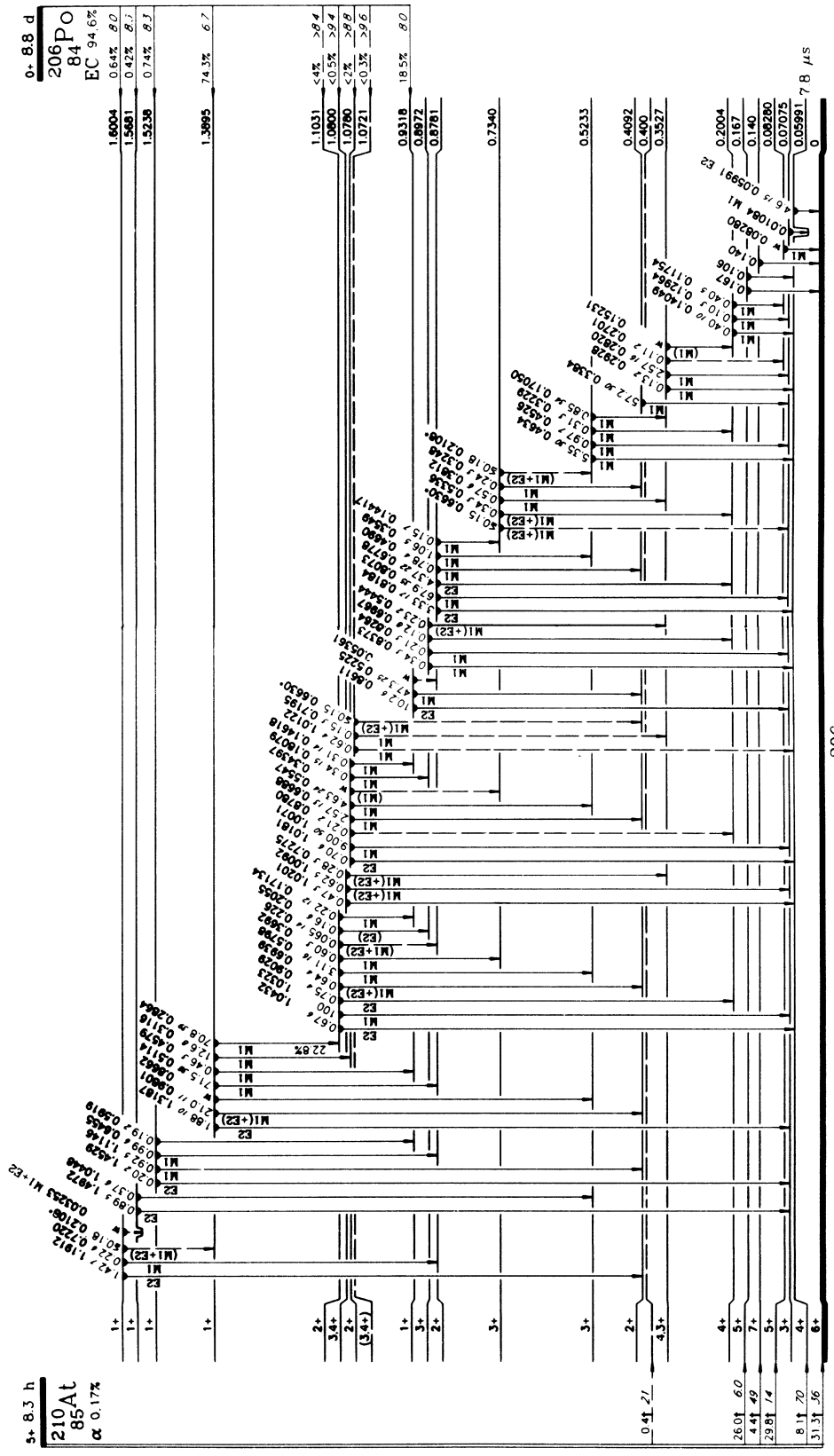

FIG. 4. Level scheme of ^{206}Bi. Relative photon intensities (with errors in italics) from the ^{206}Po decay are shown above the transitions. Relative α intensities from the ^{210}At decay and calculated (Ref. 19) α hindrance factors are also shown. The absolute intensity of the 286.4-keV γ ray was calculated from the level scheme to be 22.8 ± 2.0 photons per 100 decays of ^{206}Po.

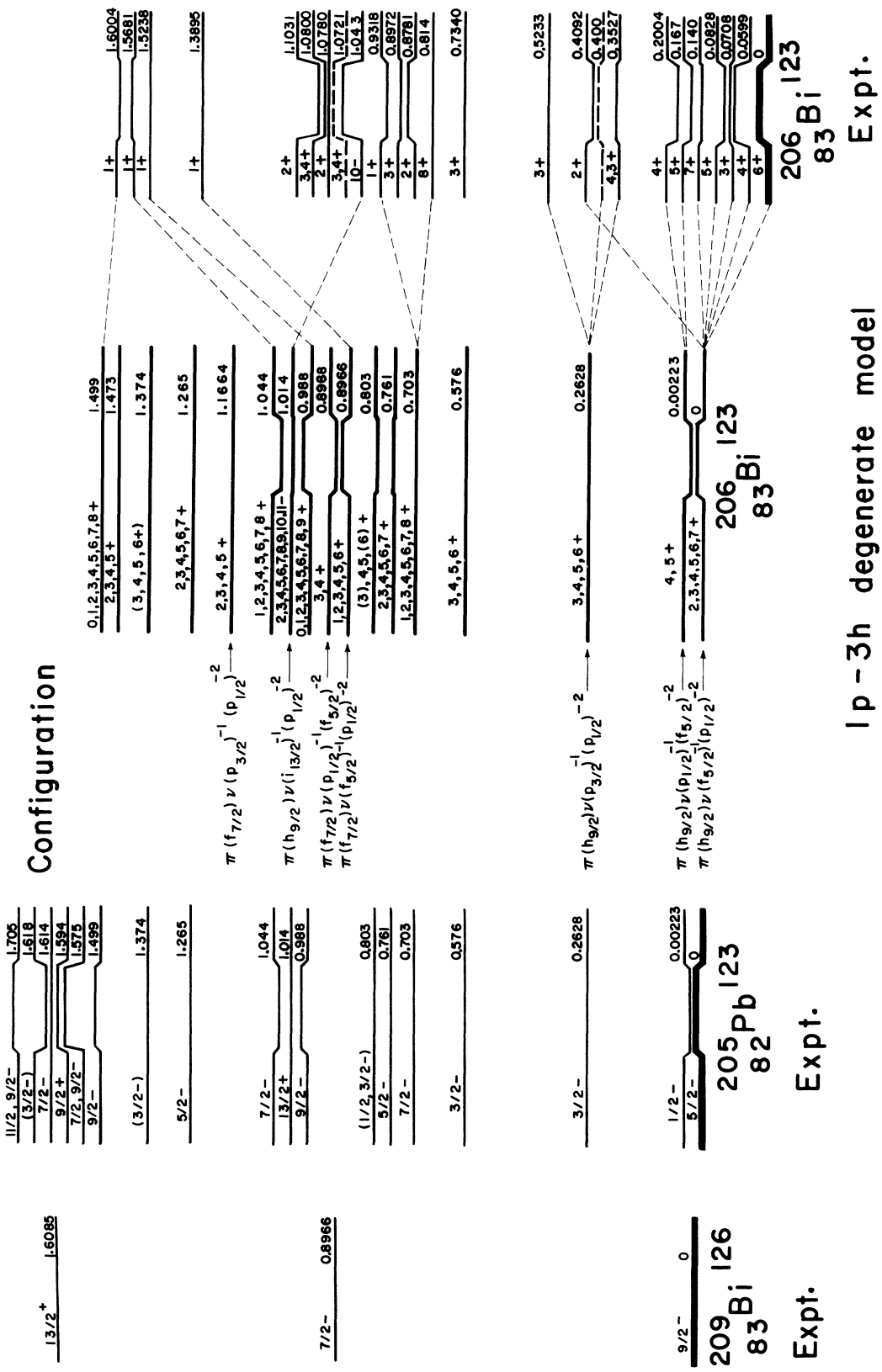

FIG. 5. Comparison of the experimental (Refs. 1–9) ^{206}Bi level scheme with the predictions of a simple coupling model. The experimental (Refs. 21, 23) states of ^{209}Bi and ^{205}Pb are used to estimate the energies and range of spins from multiplets formed from couplings of the odd proton and the three-neutron holes (1p-3h states) in ^{206}Bi.

theoretical α-rate calculations.[7]

A state at 83 ± 1 keV that is deexcited by a γ-ray transition to the ground state has been identified[6] in the α decay of ^{210}At. Theoretical α-rate calculations of Ref. 7 suggested an assignment of 5^+. An 82.80-keV $M1$ transition observed by Ref. 9 has been placed in Fig. 4 as deexciting this state, employing the fact that the 117.5-keV transition (which feeds the 82.8-keV state) is in coincidence with the 511.4 and 677.8 keV transitions. This is shown in Figs. 2(c) and 3(d). The weak intensity of the 82.8-keV γ ray, compared to the K x rays, prevented the observation of this transition in the γ-ray singles measurements. The intensity balance of the decay scheme is also consistent with this placement.

A 7^+ state at 140 keV was observed in in-beam experiments[3,4] and the α decay[5,6] of ^{210}At. It decays by a 140 ± 1-keV $M1$ transition to the ground state. The 140.5-keV $M1$ transition observed in the electron-capture decay of ^{206}Po has not been placed as deexciting this level. A 7^+ state should not be populated with such an intensity, if at all, in the electron-capture decay. Further, the γ-γ coincidence data (Figs. 2c and 3d) are only consistent with the placement of the 140.5-keV γ ray as depopulating the 200.4-keV level.

Coincidence relations of Table II define a state at 409.2 keV. A 2^+ assignment can be made for this state from the $M1$ multipolarities of the 338.4-keV transition to the 3^+ state at 70.8 keV and the 980.1-keV transition from the 1^+state at 1389.5 keV.

As indicated by the dashed lines in Fig. 5, these even parity states discussed above with spins between 2 and 7 are tentatively assigned the dominant configuration $\pi(h_{9/2})\nu(f_{5/2})^{-1}(p_{1/2})^{-2}$. Relative α-decay rate calculations[7] assuming this configuration for these six states also gave results that are in essential agreement with experimental measurements. Even better agreement for the 4^+ and 5^+ states at 59.9 and 82.8 keV, respectively, was obtained when small admixtures from the $\pi(h_{9/2})\nu(p_{3/2})^{-1}(p_{1/2})^{-2}$ and $\pi(h_{9/2})\nu(p_{1/2})^{-1}(f_{5/2})^{-2}$ configurations were included in the description of these states.

B. Levels at 167 and 200.4 keV

Coincidence relationships define a state at 200.4 keV. The three $M1$ transitions depopulating this state to the 4^+, 3^+, and 5^+ states at 59.9, 70.8, and 82.8 keV, respectively, establish the spin and parity as 4^+.

There is no definite evidence from our γ-ray measurements that the 5^+ state at 167 ± 1 keV identified[5,6] in the α decay of ^{210}At is also populated in the ^{206}Po electron-capture decay. Reference 6 observed two transitions of 106 ± 1 and 167 ± 2 keV [with the relative photon ratio of (1.6 ± 0.5)/1.0] depopulating this state, but neither was observed in our measurements.

If these two states are identified with the shell-model $\pi(h_{9/2})\nu(p_{1/2})^{-1}(f_{5/2})^{-2}$ configuration as indicated in Fig. 5, then the 167-keV state must be the 5^+ member of this configuration. Theoretical (relative) α-decay rates and electromagnetic transition rates employing these assignments were in agreement with experimental results, provided appreciable admixtures of the $\pi(h_{9/2})\nu(f_{5/2})^{-1}(p_{1/2})^{-2}$ and $\pi(h_{9/2})\nu(p_{3/2})^{-1}(p_{1/2})^{-2}$ configurations were also included in the wave functions.[6,7]

C. Levels at 352.7, (400), and 523.3 keV

The states at 352.7 and 523.3 keV are well defined by coincidence and sum-difference relationships. The $M1$ transitions of 292.8 and 282.0 keV from the 352.7-keV state to the 4^+ and 3^+ states at 59.9 and 70.8 keV, respectively, limit the spin of this state to 4 or 3 only. A weak argument, like lack of $M1$ transitions feeding this state from higher-lying 2^+ states, can be used to make a tentative assignment of 4^+ more favorable, but speculative.

The transitions not observed would be of $E2$ multipolarity in comparison with the faster $M1$ transitions which are observed to populate lower-lying 3^+ states. A spin and parity assignment of 3^+ for the state at 523.3 keV can be made on the basis of the $M1$ character of the 463.4-keV transition deexciting this state to the 4^+ state at 59.9 keV and by population of this state by an $M1$ transition of 554.7 keV from the 2^+ state at 1078.0 keV.

A tentative state at 400 ± 3 keV has been identified[5] in the α decay of ^{210}At. There is no additional data about its γ-decay properties. However, the energy of this state does not agree with the energy of the 2^+ state at 409.2 ± 0.2 keV. Further, theoretical α-rate calculations[7] do not predict such an intensity for the population of the configuration $(\pi(h_{9/2})\nu(f_{5/2})^{-1}(p_{1/2})^{-2})_{2^+}$. Thus it is believed that these are two separate states. One might argue that the state at 400 keV is a 5^+ state which is populated by an admixture of the favored α decay configuration. If this is so, one can make tentative assignments for the dominant configurations of these states as $(\pi(h_{9/2})\nu(p_{3/2})^{-1}(p_{1/2})^{-2})_{3,4,5,6^+}$. This would imply that a yet unobserved 6^+ state also exists in this energy region. Such a state is not expected to be populated by the electron-capture decay of ^{206}Po. We have indicated these tentative assignments in Fig. 5.

D. Levels at 734.0, 878.1, 897.2, 1072.1, 1078.0, 1080.0, and 1103.1 keV

The level at 734.0 keV is defined by numerous sum-difference relations and by the coincidence relations of the 282.0 - and 381.2-keV transitions shown in Table II. The $M1$ transitions of 533.6 and 328.8 keV to the 4^+ and 2^+ states at 200.4 and 409.2 keV define the spin and parity as 3^+.

States at 878.1, 1078.0, and 1103.1 keV are very well defined by coincidence relations shown in Table II. A definite spin and parity assignment of 2^+ for each of these three states can be made since each state is populated by an $M1$ transition from the 1^+ state at 1389.5 keV and each decays by an $E2$ transition to the 4^+ state at 59.9 keV. The lack of β-decay feeding to these states is also consistent with second-forbidden transitions[26] implied by the 2^+ assignment.

Coincidence relationships among γ rays establish a state at 897.2 keV. An assignment of 3^+ for the state can be made because of the 180.79-keV $M1$ transition populating it from the 2^+ state at 1078.0 keV and the 837.3-keV $M1$ transition depopulating it to the 4^+ state at 59.9 keV.

The states at 1072.1 and 1080.0 keV are established only by a limited number of sum-difference relationships indicated by the decay scheme of Fig. 4. If the transitions are placed correctly, the multipolarities limit the spin to 3 or 4 and the parity as even. No γ-ray transitions could be placed populating these states, implying that a weak electron-capture feeding to these states apparently exists. However, decay to states of these spins would be third forbidden, or greater. Such decays are not expected to compete with the allowed decay branches to the 1^+ states. Thus it is almost certain that weak, unplaced, or unobserved transitions populate these two states and are the cause of these apparent feedings. In Fig. 4 we show dashed feedings for these states with the indicated limits representing the intensities of such transitions.

E. Levels at 931.8, 1389.5, 1523.8, 1568.1 and 1600.4 keV

States at 931.8 and 1389.5 keV are firmly established from coincidence realtions of Table II. The state at 931.8 keV can be given a spin and parity assignment of 1^+ because of the 861.1-keV $E2$ transition to the 3^+ state and the 522.5-keV $M1$ transition to the 2^+ state at 409.2 keV. In addition, the logft value of 8.0 for decay to this state is also consistent with a spin of 1 as all known second forbidden (nonunique) transitions[26] have values of log$ft \gtrsim 11.0$. The state at 1389.5 keV receives about 77% of the total electron-capture decay. The 1318.7 keV $E2$ transition to the 3^+ state at 70.8 keV and the 511.4 keV $M1$ transition to the 2^+ state at 818.1 keV make a spin and parity assignment of 1^+ definite. This is supported by the logft value of 6.7 which is consistent[26] only with an allowed β decay (i.e., $0^+ \rightarrow 1^+$), as no parity change is involved in the electron-capture decay.

States at 1523.8 and 1600.4 keV are established by the coincidence of the 338.4-keV transition with the 1114.6- and 1191.2-keV γ rays, respectively, as shown in Fig. 2. The $E2$ transition to the 3^+ state at 70.8 keV and the $M1$ transition to the 2^+ state at 409.2 keV established the spin and parity of the 1532.8-keV state as 1^+; the logft value is also consistent with an allowed transition. The logft value of 8.0 for decay to the state at 1600.4 keV is the strongest argument for a 1^+ assignment as the multipolarities of the 1191.2 - and 222.0 -keV transitions can only limit the spin assignments to 1, 2, or 3.

Coincidence data for the 1497.2 - and 1044.8-keV transitions are consistent with a state at 1568.1 keV. The parity is established as even by the 1497.2-keV $E2$ transition to the 3^+ state at 70.8 keV. Again the logft value of 8.4 indicates an allowed transition, thereby strongly arguing for a spin and parity assignment of 1^+.

V. DISCUSSION

The rather low Q value for the electron-capture decay of ^{206}Po helps to make an interpretation of the levels of ^{206}Bi easier, as only five states receive any measureable direct electron-capture decay in the present level scheme. Electron-capture decays to these 1^+ states from the even-even 0^+ ground state of ^{206}Po proceed via an allowed β transition. Subsequent γ-ray decay of these 1^+ states populates states of spin 2, 3, 4, and 5 until the 6^+ ground state is reached.

In Fig. 5 we have shown five possible (degenerate) multiplets formed from couplings of the odd proton and the odd neutron (or three-neutron holes) that give rise to 1^+ states in the energy range < 1500 keV. (It may only be fortuitous that five 1^+ states are presently experimentally identified.) The 1^+ state at 1389.5 keV receives most of the electron-capture decay and is believed to arise from the coupling of a $2f_{7/2}$ proton to the three-neutron holes with a configuration of the ground state of ^{205}Pb. This is indicated in Fig. 5. Such a configuration of ^{206}Bi can be written explicitly as $(\pi(f_{7/2})\nu(f_{5/2})^{-1}(p_{1/2})^{-2})_{1^+}$. The 0^+ ground state of ^{206}Po is of a two proton-four neutron hole character with the probable dominant configuration $(\pi(h_{9/2})^2\nu(f_{5/2})^{-2}(p_{1/2})^{-2})_{0^+}$. An allowed single-particle electron-capture decay of the type $\pi 2f_{7/2} \xrightarrow{EC} \nu 2f_{5/2}$ can be used to explain the electron-

capture decay to the 1^+ state at 1389.5 keV if the ground state wave function of ^{206}Po has a second component of the form $(\pi(f_{7/2})^2\nu(f_{5/2})^{-2}(p_{1/2})^{-2})_{0^+}$. This same type of argument has been used[27,28] to explain the electron-capture decay of ^{207}Po and ^{205}Po to the $\frac{7}{2}^-$ single-particle states in ^{207}Bi and ^{205}Bi, respectively. Reference 9 has previously suggested this type of mechanism for ^{206}Po and we also believe that this is the main mechanism for the electron-capture decay. Decay to the other 1^+ states in ^{206}Bi (with somewhat higher logft values) probably proceeds via the same single-particle mechanism through admixtures of the $(\pi(f_{7/2})\nu(f_{5/2})^{-1}(p_{1/2})^{-2})_{1^+}$ configuration present in the wave functions of these states.

States assigned to the $(\pi(h_{9/2})\nu(f_{5/2})^{-1}(p_{1/2})^{-2})_{2,3,4,5,6,7^+}$, $(\pi(h_{9/2})\nu(p_{1/2})^{-1}(f_{5/2})^{-2})_{4,5^+}$, and $(\pi(h_{9/2})\nu(p_{3/2})^{-1}(p_{1/2})^{-2})_{3,4,5,6^+}$ configuration have been previously discussed in Sec. IV, and are shown in Fig. 5. Calculations of electromagnetic transition probabilities and α decay rates using these assumed configurations for states of ^{206}Bi populated in the α decay of ^{210}At have previously been made.[6,7] The results indicated that agreement of the theoretical calculations with existing experimental data could be obtained if some configuration mixing among these three configurations was allowed for the 4^+ and 5^+ states.

Finally, the states in the energy range of 734.0 to 1103.1 keV are presumably of a rather complex structure and we presently cannot ascribe a specific configuration to these states using only qualitative arguments. However, two states observed[3,4] in recent in-beam experiments in this energy range merit some additional remarks. A 10^- isomer of 1 msec half-life at 1043 keV has been assigned[29,30] a $\pi(h_{9/2})\nu(i_{13/2})^{-1}(p_{1/2})^{-2}$ configuration. This is also consistent with the qualitative predictions of Fig. 5. Decay of this isomeric state to an 8^+ state at 814 keV has been observed. This 8^+ state, as suggested from Fig. 5, might arise from a coupling of a $1h_{9/2}$ proton with a $\frac{7}{2}^-$ state of ^{205}Pb. The dominant configuration of the $\frac{7}{2}^-$ state of ^{205}Pb is expected to be of the type $(\nu(f_{5/2})^{-2}(p_{1/2})^{-1})_{7/2^-}$, with perhaps the internal coupling $(\nu(f_{5/2})^{-1}(p_{1/2})^{-1})_{2^+}(f_{5/2})^{-1})_{7/2^-}$. Thus the 8^+ state of ^{206}Bi might have a major component of the type $(\pi(h_{9/2})(\nu(f_{5/2})^{-2}(p_{1/2})^{-1})_{7/2^-})_{8^+}$. Perhaps these latter two states provide further evidence that the level structure of ^{206}Bi can be interpreted in terms of one particle-three hole configurations, at least up to 1389 keV.

Note added in proof: Kanbe, Fujioka, and Hisatake have recently published[31,32] the results of their conversion electron work.[9] Their proposed decay scheme is in essential agreement with that of this work.

ACKNOWLEDGMENTS

We are grateful to Dr. K. Hisatake and Dr. M. Kanbe for providing us with their (internal conversion-electron) data prior to its publication. We also wish to acknowledge Mr. A. Al-Nasser for assistance in analysis of some of the data.

---

*This work prepared under the auspices of the U.S. Atomic Energy Commission.

†Present address: Argonne National Laboratory, Chemical Engineering Division, Argonne, Illinois 60439.

‡Permanent address: Department of Physics, Kuwait University, El-Kuwait, Kuwait.

[1]E. Arbman, Nucl. Phys. 3, 625 (1957).

[2]A. W. Stoner, University of California Radiation Laboratory Report No. UCRL-3471, 1956 (unpublished).

[3]Yu. N. Rakivnenko *et al.*, Ukr. Fiz. Zh. 17, 1037 (1972).

[4]U. Hagemann, K. H. Kaun, W. Neubert, W. Schulze, and F. Stary, Nucl. Phys. A197, 111 (1972).

[5]N. A. Golovkov, Sh. Guetkh, B. S. Dzhelepov, Yu. V. Norseev, V. A. Khalkin, and V. G. Chumin, Izv. Akad. Nauk, SSSR Ser. Fiz. 33, 1622 (1969) [Bull. Acad. Sci., USSR Phys. Ser. 33, 1622 (1970)].

[6]L. J. Jardine and A. A. Shihab-Eldin, Nucl. Phys. A244, 34 (1975).

[7]A. A. Shihab-Eldin, L. J. Jardine, and J. O. Rasmussen, Nucl. Phys. A244, 435 (1975).

[8]L. J. Jardine and A. A. Shihab-Eldin, Bull. Am. Phys. Soc. 18, 1379 (1973).

[9]M. Fujioka, M. Kanbe, and K. Hisatake, Phys. Rev. Lett. 31, 114 (1973); K. Hisatake and M. Kanbe (private communication).

[10]P. E. Figgins, National Academy of Sciences, National Research Council Report No. NAS-NS-3037, 41, 1961 (unpublished).

[11]L. J. Jardine, S. G. Prussin, and J. M. Hollander, Nucl. Phys. A190, 261 (1972).

[12]L. J. Jardine, University of California Lawrence Berkeley Laboratory Report No. LBL-246, 1971 (unpublished).

[13]J. R. Routti and S. G. Prussin, Nucl. Instrum. Methods 72, 125 (1969).

[14]L. J. Jardine, University of California Radiation Laboratory Report No. UCRL-20476, 1971 (unpublished).

[15]L. J. Jardine, Nucl. Instrum. Methods 96, 259 (1971).

[16]R. S. Hager and E. C. Seltzer, Nucl. Data A4, 1 (1968).

[17]Y. Le Beyec and M. Lefort, Nucl. Phys. A99, 131 (1967).

[18]A. H. Wapstra and N. B. Gove, Nucl. Data A9, 267 (1971).

[19]C. M. Lederer, University of California Lawrence Berkeley Laboratory Report No. LBL-1996, 1973 (unpublished).
[20]E. J. Konopinski and M. E. Rose, in *Alpha-, Beta-, and Gamma-Ray Spectroscopy*, edited by K. Siegbahn (North-Holland, Amsterdam, 1965), Vol. 2, p. 1357.
[21]M. J. Martin, Nucl. Data B5, 287 (1971).
[22]M. R. Schmorak, Nucl. Data B6, 425 (1971).
[23]J. H. Hamilton, V. Ananthakrishnan, A. U. Ramayya, W. M. LaCasse, D. C. Camp, J. J. Pinajian, L. H. Kern, and J. C. Manthuruthil, Phys. Rev. C 6, 1265 (1972).
[24]I. Lindgren and L. M. Johansson, Ark. Fys. 15, 445 (1959).
[25]E. Arbman and P. A. Tove, Ark. Fys. 13, 61 (1958).
[26]S. Raman and N. B. Gove, Phys. Rev. C 7, 1996 (1973).
[27]P. K. Hopke, R. A. Naumann, and E. H. Spejewski, Phys. Rev. 187, 1709 (1969).
[28]M. Alpsten and G. Astner, Nucl. Phys. A134, 407 (1969).
[29]G. Schäfer, H. Hübel, C. Günther, A. Goldman, and D. Riegel, Phys. Lett. B 46B, 65 (1973).
[30]T. W. Conlon, Nucl. Phys. A212, 531 (1973).
[31]M. Kanbe, M. Fujioka, and K. Hisatake, J. Phys. Soc. Jpn. 38, 928 (1975).
[32]M. Kanbe, M. Fujioka, and K. Hisatake, J. Phys. Soc. Jpn. 38, 917 (1975).